Light Metals 2015

ALUMINUM REDUCTION TECHNOLOGY

Operations and Energy Consumption

SESSION CHAIR
Claude Fradet
Rio Tinto Alcan
Jonquiere, Quebec, Canada

On-line Monitoring of Individual Anode Currents to Understand
and Improve the Process Control at Alouette

Lukas Dion[1,3], Charles-Luc Lagacé[1], James W. Evans[2], Ron Victor[2] and Laszlo I. Kiss[3]

[1] Aluminerie Alouette inc. 400 chemin de la Pointe-Noire, C.P. 1650, Sept-Îles, QC, G4R 5M9, CANADA
[2] Wireless Industrial Technologies (WIT), 4096 Piedmont Ave. #193, Oakland, CA 94611, USA
[3] Aluminium Research Centre-REGAL, Université du Québec à Chicoutimi, 555 boulevard de l'Université, Chicoutimi, QC, G7H 2B1, CANADA

Keywords: WIT, anode current, anode effect detection, alumina distribution, cell instability

Abstract

In 2014, Alouette acquired a system to monitor the on-line anode current on two pots. This system, developed and supplied by WIT, reports all anodes current and the pot voltage for every second of operation. The following paper describes some of the resulting improvements that apply to the process control of the aluminum electrolysis cell.

Current monitoring of the anodes easily indicates the generation of localized anode effects (AE) prior to their propagation into a "voltage triggered" AE. Basic concepts, algorithms, results and optimization to improve the detection rate are discussed in the first part of the paper.

Moreover, AE are directly influenced by the alumina distribution in the cell. A better understanding of the dissolution patterns based on the feeder's position was achieved by using the monitoring system.

Introduction

Aluminerie Alouette, located in Sept-Îles, Québec, is the largest aluminum smelter in the Americas with a capacity of over 600,000 tons per year. Wireless Industrial Technologies (WIT), is a small company in Oakland, California, incorporated in 2005 to develop wireless technology for application in heavy industry.
In January, 2014 Alouette acquired a system from WIT for monitoring the current of individual anodes on two pots. The objective was to determine whether anode current monitoring could provide early warning of anode effects or bring other benefits to pot operation and fundamental understandings.

The anode current measurement system

The currents in every anode rod was measured every second using a system developed by Wireless Industrial Technologies (WIT). The system has been described in previous publications [1, 2] and will be only briefly described here. The WIT system relies on measuring the magnetic field developed by the current flowing in the anode rod. Two Hall effect sensors are incorporated in a circuit, called a "slave" placed next to each anode rod. The slaves are wired along a single cable to one of two "masters" that are placed at the end of the pot. The cable serves to both bring power to the slaves and as a route for data to flow to the masters, which then relay the data wirelessly to a receiving computer ("manager") and thence to the cloud for processing. Data were made available through the internet in the form of a "dashboard" where real-time currents, pot voltage and slave temperatures were plotted for password controlled access from anywhere. Use of two sensors and mathematical modeling enable "crosstalk" from currents in other anode rods, risers etc. to be eliminated. The model also permits the conversion of magnetic field measurements into actual currents although the former are adequate surrogates for most purposes. There were marginal differences between the installation at Alouette and those at other smelters except for a more rugged arrangement for mounting the slaves. The slaves were mounted in stainless steel "enclosures" that were then bolted to a rectangular stainless steel tube that was readily mounted underneath the anode bus. Fig. 1 is a photo of the tubes (upside down), each section carrying two slaves, prior to shipment to Alouette.

Fig. 1 Slaves, insulated and fixed to rectangular tubing for mounting underneath the anode bus (shown upside down before shipment from WIT)

Anode effect detection

It is now well known that in the few seconds or minutes before the voltage increase of an anode effect (AE) the anode currents start to redistribute [2, 3]. This redistribution therefore provides an early warning of an imminent AE that might be exploited to minimize or avoid AEs. Fig. 2 shows this rearrangement for an AE at Alouette on June 16th, 2014. The currents (represented here by the magnetic fields that they generate) start to deviate significantly from their

previous values about three minutes before the rapid voltage increase of the AE.
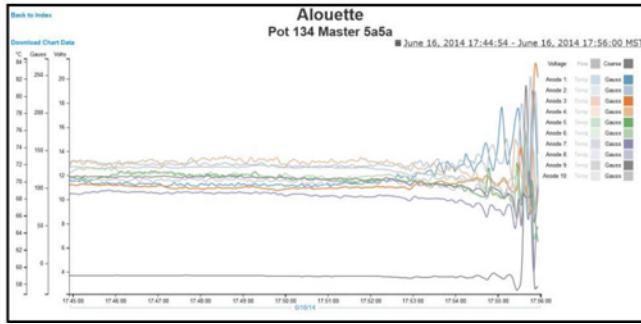
Fig. 2: Dashboard plot of magnetic fields (representing individual anode currents) and pot voltage in the minutes prior to an anode effect.

Unfortunately the onset of an AE is not always as clear cut as depicted in Fig. 2. Pot operations such as anode changes or phenomena such as pot instability can obscure the redistribution of current that precedes an AE. Furthermore, human observation of the traces such as those in Fig. 2 is impractical for a potroom of a few hundred pots. Consequently an algorithm for "automatic" recognition of imminent AEs was required. The algorithm that was developed works by comparing short term and long term moving averages for the field from each anode current. Regarding Fig. 2 it is clear that a moving average over, say, 20 seconds will start to deviate from an average over 20 minutes at about the time that the human eye would recognize the redistribution leading up to an AE. The algorithm was constructed to register an event when the change in the short term average was a significant fraction of the long term average. The algorithm kept track of how many anodes were manifesting such events; when that number exceeded a few (say two or three anodes) then an AE alert was communicated to Alouette through the internet.

The performance of the system and the algorithm were evaluated over a period of a few weeks in the summer of 2014. During this period, 97 AEs occurred on the two pots as recorded by routine voltage measurements by Alouette. The various parameters of the algorithm (e.g. length of time of the short term average) were crudely optimized based on intuition and preliminary data. The intent was to provide alarms for imminent AEs with as few false alarms as possible. The ultimate goal is to link the alarms directly into the pot control system.

Fig. 3 shows the results from the test for two different sets of parameter. Of the 97 AEs that occurred, the system detected more than two thirds in both cases, although a few detections were after the voltage increase. The results also demonstrate that more sensitivity (algorithm 2) leads to fewer missed anode effect but to a significant increase in false alarms.
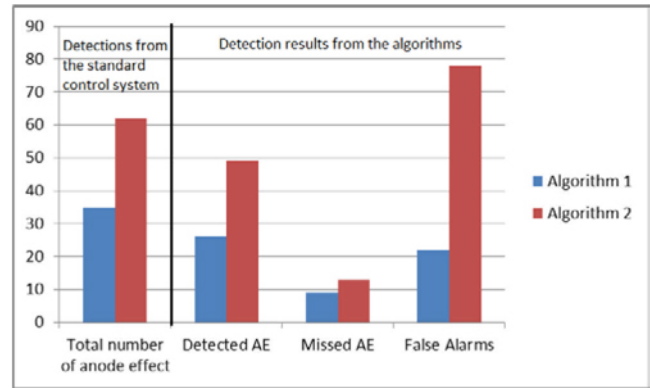
Fig. 3 : Algorithms efficiency of detection

Fig. 4 shows how many of these false alarms were caused by anode changes, pot instability etc. The figure also reports the distribution of warning times. Many AEs were detected five minutes or less before the voltage surge, a few between 5 minutes and 15 minutes and a the majority of the detections were prior to 15 minutes. The reliability of the alarms from the last category was questioned at first. Further analysis indicated that a specific type of instability was related to an alumina feeding problem which eventually leads to an anode effect. Those instabilities are in fact pseudo-anode effects caused by a localized lack of alumina. This phenomenon appears to be more present in the low ACD cells because of the smaller volume of bath. A good treatment protocol as a follow-up to the alarms should improve the overall performances of the cells on both short and long-term average.
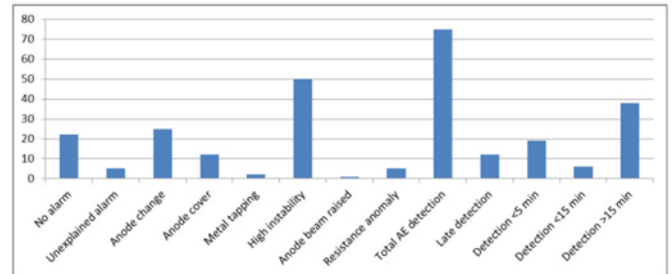
Fig. 4 : False alarm and detection time prior to AE. Both algorithms included.

It is anticipated that the algorithm can be improved in three ways: optimization of the four parameters mentioned in the penultimate paragraph (short term moving average, long term moving average, deviation ratio and number of anodes deviating), use of other statistical measures of change as well as incorporation of additional cell data such as voltage noise.

Understanding the alumina distribution in the cell

<u>Previous work</u>

Based on the general consensus, and in agreement with the results above, it is evident that a good alumina distribution in the cell will lead to a lower number of anode effects. The alumina feedings of the cells are regulated by a controller. Actions are applied based on the bath resistance variations over time, assuming that most of these variations are consequent of a change in the alumina concentration. It is commonly known that the resistance changes non-linearly as the alumina % changes; with an exponential increase as the concentration becomes very low. Kvande et al.[4]

illustrated this curve based on numerous in-cell measurements for a 175 kA pre-baked cell using a pseudo-resistance which reflect the electrolysis bath portion of the overall cell's resistance. The absolute value of the pseudo-resistance might change with the technologies, but the shape of the curve remains similar.
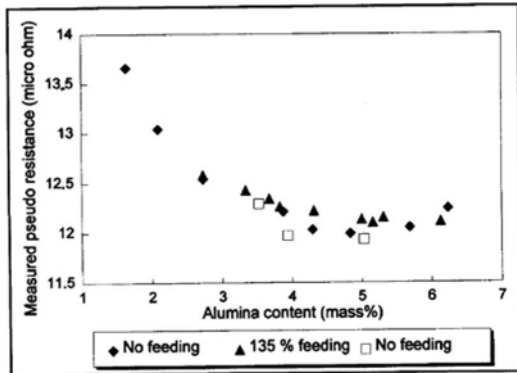
Fig. 5 : Pseudo-resistance as a function of alumina content for a 175 kA prebake cell. [4]

The pseudo-resistance is only representative of the overall concentration in the cell and it is hardly possible to identify a localized concentration without further tools. Moreover, it is very difficult to investigate the alumina distribution pattern in the cell because of the corrosive behavior of the electrolysis bath. A possible option to investigate requires taking discrete samples or measurement on special locations in the cell. This hard task can give information, but it is not equivalent to a timely follow-up. The results discussed further in this paper illustrate a first step towards understanding the alumina distribution in the cell based on on-line anode current monitoring.

Movements of the liquid (Magneto-hydro-dynamics (MHD)) in cells has been studied numerically for many years but the alumina distribution in the bath is rarely included in those simulations due to the complexity of such a model. The bath flow and the dissolved alumina within are influenced by four main mechanisms [5]:
- Release of gas beneath the anodes (bubble flow)
- Drag exerted by the metal on the bath and *vice versa*
- Interaction of the magnetic and electric currents in the bath and metal
- Thermal convection

Moreover, the alumina concentration in the bath is influenced by other mechanisms as well:
- Electrolysis of the alumina to produce aluminium
- Discrete feeding points and feeding periods
- Dissolution speed of alumina agglomerates
- Re-oxidation of the aluminium in the cells
- Vertical movements of the alumina sludge, from aluminium to electrolysis bath.

Feng et al. [6] performed a computational fluid dynamics modeling of the alumina distribution and results of this simulation are clear on the fact that non-uniformity is present in both horizontal axes of the cell. The highest concentrations of alumina are closest to the feeders and to the cell extremities.

An extensive numerical simulation was performed by Hofer [7], taking most of the mechanisms into account and validating the simulation using simultaneous sampling in nine different locations of the electrolysis cell. His study indicates that on stable operation, the alumina concentration is periodic in time. The results clearly indicate that a difference in the alumina concentration (± 0.3 %) is observed between the average and individual positions concentrations points.

Moxnes et al. [8] considered this non-uniformity in the concentration and successfully redistributed the alumina doses from the different feeders to achieve a more uniform concentration. Their results indicate better cell performances (lower number of anode effects, higher current efficiency, current more uniformly distributed and more). Current pick-up of individual anodes, combined with large additions of aluminium fluoride was used to determine the influence of the different feeding position.

Impact of each feeder on the alumina distribution

The aim of this study was to understand which areas of the cells are supplied by each feeder. A good understanding makes it possible to identify overlapping zones (risk of creating sludge) and the areas where a lack of alumina might be expected (risk of generating pseudo anode effect (PAE)). As mentioned in a previous paper by Coursol and al. [9], Alouette operation standards are very close to the critical interpolar distance. A good control of the feeding is therefore much more important, as the total volume of bath below the anode containing alumina has become very small.

To achieve our goal, several tests were performed on two AP40LE prebake cells operating above 390 kA. The testing was based on the assumption that local alumina concentration will have an influence on individual anode current measurements. Using the system provided by WIT, it would be possible to distinguish a low alumina concentration (lower anode current) from a normal or high alumina concentration (higher anode current to compensate).

During the tests, three out of the four feeders of each cell were stopped and only one feeder was left to provide alumina for the entire cell. The exact location for the main alumina input was known and no external perturbations were allowed during the testing (anode beam movements, anode changes, crust breaking, bath or metal tapping, etc.). The feeders were stopped until the voltage increase was exponential and up to the point where an anode effect was imminent. At this point, all feeders were restarted and data were compiled. All the tests were performed only if the cell behavior was considered stable for at least one hour before the measurements. All the feeders were also checked before stopping the feeders to make sure that feeding prior to the test was according to the standards (no clogged hole, etc.).
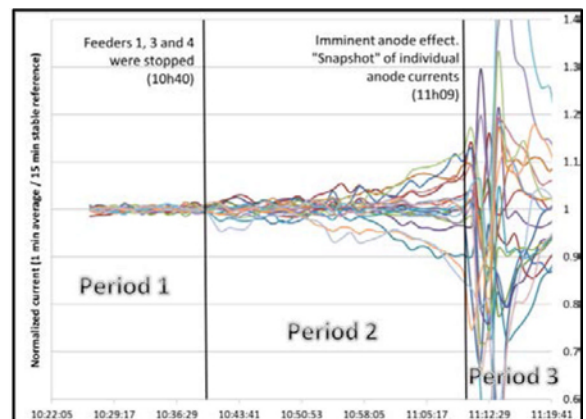
Fig. 6: Test performed on cell B134, on August 13th 2014. Feeder 2 was the only one feeding.

Fig 6. illustrates the results based on one-minute average for every anode. Three periods are illustrated on the figure based on the measurements.

- Period 1 (stable period): During fifteen minutes prior to stopping the feeders, the current is monitored for each individual anode and an average value for each anode is calculated. These current values are the reference to which each anode is normalized. Therefore a value of 1 indicated that the anode current is the same as in normal operation.
- Period 2 (testing period): This period covers the time lapse where the cell feeding is unusual (one feeder); from the time feeders were stopped up to the point where they were restarted. The "snapshot" point for the current evolution is considered two minutes before the time when the feeders were restarted. Based on the experimentation, this two minute window is sufficient to avoid perturbations caused by the pseudo-anode effects in most cases.
- Period 3 (back to normal period): This period merely illustrates the instability occurred in the cell by lack of alumina and the going back to a normal slope of the anode currents as the feeding has been resumed.

A minimum of 8 tests were performed for each feeder to increase the statistical reliability of the results. 33 tests were performed and out of the 660 anode currents measured in the "snapshot", only 3 values were discarded due to overheating of the slave during the period 2, leading to uncertainty in the values reported. Results for each feeder are illustrated in the next figures.
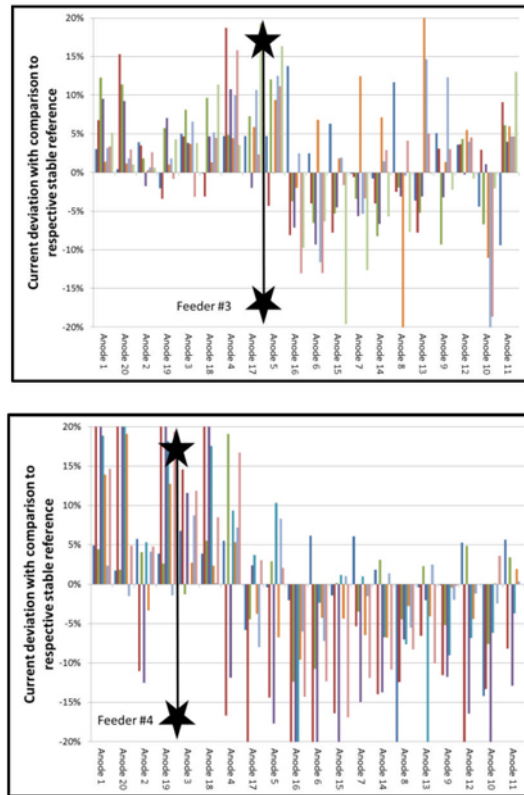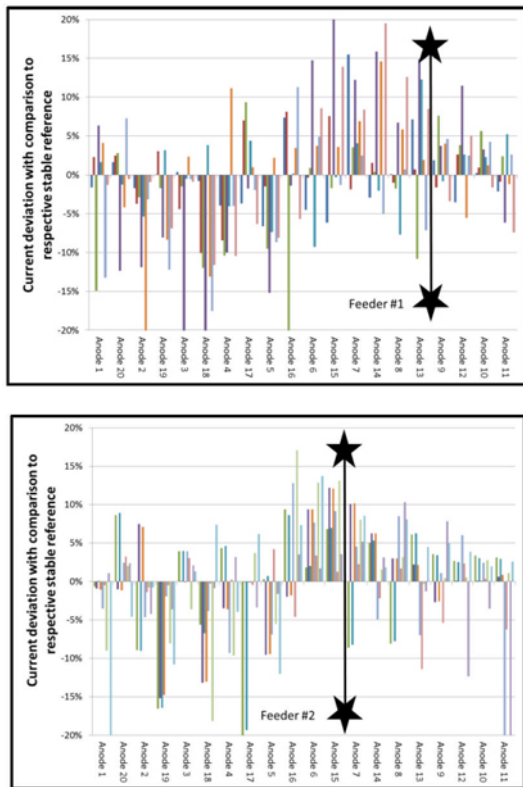
Fig. 7, 8, 9 and 10 : Current deviation based on anode position relative to alumina input position.
Feeder 1 to feeder 4 respectively.

The histograms illustrate the results of every test performed based on the position of the working feeder (2 stars joined by a vertical line). Anode numbering on the figures is representative of their relative position from duct end (left) to tapping end (right) but no considerations are made for upstream (1 to 10) and downstream (11 to 20). Values reported in the histogram represent the current deviation observed between the "snapshot" and the respective reference from the stable period. A positive value indicates that the anode was picking up more current at that time than it was prior to the test.

For each feeder, a repetitive behavior can be observed based on the several tests performed. It is safe to believe that this behavior represents the zone of the cells which is well fed by the respective feeder. The results are consistent with the double loop pattern described in many of the MHD publications, especially the metal velocity vectors described by Severo et al. [10] The frontier region of both the loop appears to be slightly shifted towards the duct end if we closely consider the results of all the feeders.

It was possible to compile the results of all four feeders to give a clearer idea of the alumina concentration during normal operations when the feeding is performed equally across all the cells. For all feeder positions, we assume that the same amount of alumina is fed, reaches the electrolytic bath and is quickly dissolved. By looking at the average value for each anode positions for each of the four scenarios, if the average current pick up was higher than 3%, a (+) was added to the respective anode, which signifies that the alumina from one feeder reaches this anode easily. On the other hand, when the average current was lower than 3%, a (-) was added to the

respective anode indicating that this anode position is likely to lack alumina if the respective feeder that should feed it has a problem. It also indicates that during normal operation, no alumina is expected to be received from a faraway feeder.

For example, by looking at anode 7 on Fig. 11, we can interpret that a significant amount of alumina is provided from the feeder #1 and #2 but no alumina is expected to be received from feeder #4.
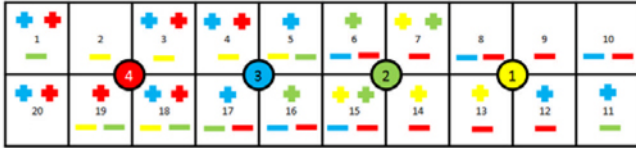
Fig. 11: Expected alumina concentration in the bath during normal feeding based on the results provided from individual feeders.

Results from the previous figure are coherent with the geometry of the cell but some observations deviate from the expectations.

A significant difference between the upstream and downstream side of the cell can be observed when investigating the specific feeders associated to each anodes. On the downstream side, there is at least one feeder associated with every anode. However, on the upstream side four anodes were not directly affected by a specific feeder suggesting that they are influenced by the overall concentration of the bath and less affected by one feeder individually. The metal pad orientation and velocity are coherent with the results from anode 8, 9 and 10 and explains part of the results. On the other hand, it is unclear why anode 2 has no associated feeder. The alumina distribution pattern appears uniform both from feeders 3 and 4 on the duct end of the cell. This anomaly is even more evident on Fig. 10.

The results also suggest that sludge accumulates in the extremities of the cell (position 1, 11, 12 and 20). It is the most likely phenomenon explaining why no lack of alumina was observed during the test when the most remote feeder was the only one feeding. It also partly explains why the feeder #3 appears to have an important impact on the behavior of anode 11 and 12.

Results illustrated in Fig. 11 are the first steps taken towards a more thorough investigation. The current results are sufficient to establish and test a new alumina feeding strategy based on the feeders' location. Optimization of the results can be achieved by further testing under different conditions. Finally, this analysis was performed using discrete value (+3% / 0 / -3%), it is possible to increase the complexity of the analysis to obtain more detailed results.

<u>Alumina distribution and anode current leading to an anode effect</u>

On August 27th, during the testing of cell B133 with only feeder #4 in function, bath samples were taken during the testing period to justify our main assumption and to increase our understanding of the cell's behavior. An area, next to the only working alumina feeder was sampled (anode 18) as well as the tap end of the cell (farthest place away from the feeder). A total of sixteen samples (3 initial samples (stable period) + 13 samples (testing period)) were taken on each location to illustrate the alumina behavior over time during the test. The alumina content was analyzed by gravimetric measurement at Alouette's laboratory. The results from this test are illustrated in Fig. 12.
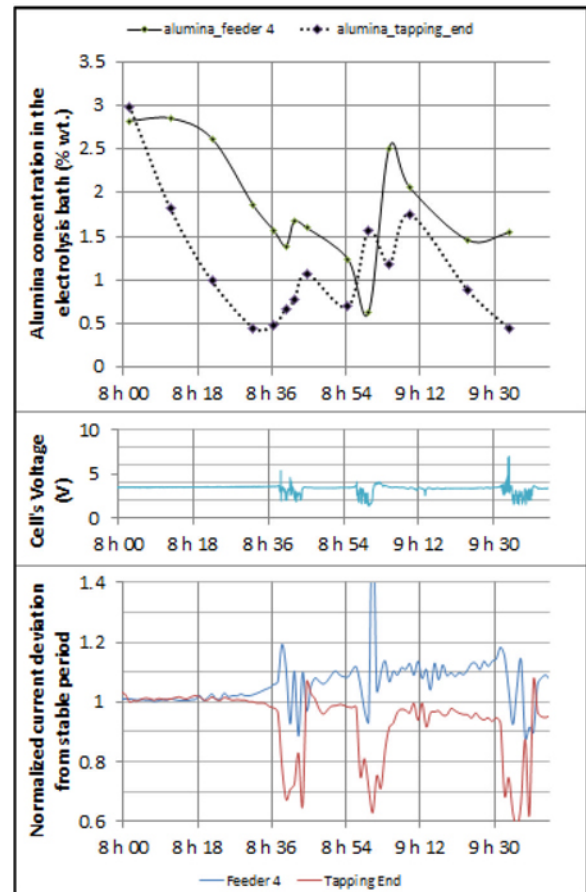
Fig. 12 : Alumina concentration, cell voltage and current deviation for the region of interest during the test period. Feeders 1, 2 and 3 were stopped at 8h00.

The current deviation illustrated in the previous figure represents the mean for the anodes nearest[1] to the zone of interest, hence anode 2, 18 and 19 for "feeder 4" and anode 9, 10, 11 and 12 for "tapping end". By investigating the correlation between these five variables during the various periods, it is possible to partly understand the behavior of the electrolysis cell, as the lack of alumina is becoming dominant in some areas of the cell.

8:00: Alumina concentration (average of 3 measurements) was measured before stopping the feeders. The concentration is similar at both sampling points.

8:00 → 8:20 : A change in the alumina concentration from the tapping end is significant, dropping approximately 1% wt. for each ten minutes. The alumina concentration near feeder 4 has not changed significantly. No change is observable for the cell voltage as well as the anode currents.

8:20→8:35 : The alumina concentration for the tapping end reaches a value below 1% wt. A significant change in the anode currents can be observed, in agreement with our assumptions.

8:35→8:44: The first instabilities in the cell voltage are noticeable. The tapping end concentration of alumina is below 0.5% wt. An important drop in current has been noticed in the tapping end region. It is very likely that a pseudo-anode effect occurred in this region of the cell creating important movement at the bath-metal interface. No action was taken to stabilize the cell.

---

[1] Anode 3 was not considered due to slave overheating.

8:45 : The alumina content of the bath increased at both sampling points. During the pseudo-anode effect, two likely mechanisms occurred explaining this increase: re-oxydation of the aluminum and movement of the cathode sludge back to the electrolytic bath.

8:54→9:05: Another instability period related to a pseudo-anode effect. The alumina concentration, for the entire cell, increased by about 1% wt.

9:05→9:32: The voltage of the cell was stable. We can notice a constant decrease in the alumina concentration for both regions. The anode current difference is more than 10% between the two groups, once again coherent with our hypothesis.

9:33 : The cell voltage increases drastically, reaching the threshold to start the anode effect treatment.

This investigation confirms three interesting facts:
1. The pseudo or real anode effects always occurred when the average alumina concentration of the cell was lower than 1% wt.
2. The first voltage instability occurred almost one hour before the real anode effect. However a lack of alumina was the root cause of this problem. It is consistent with the results of the first section of this paper (Fig. 4) assuming that our developed algorithm can detect an AE up to one hour before it occurs.
3. Irregularities in the alumina concentration, for a long period, will lead to different anode currents. This change has a negative impact on the current efficiency, especially when pseudo anode effects are reached, causing strong re-oxydation of the aluminium.

Conclusion

The WIT instrumentation, installed on two pots at Alouette, has enabled the measurement of the magnetic field, created by the current in each anode rod, every second (with few exceptions) since late January, 2014.

As observed in other smelters, and by other investigators, imminent anode effects are signaled by a redistribution of the anode currents. First steps have been taken at Alouette to use this change in currents in the "automatic" early detection of AEs so that eventually the pot control system can reduce the incidence and duration of AEs. A simple algorithm, based on short and long term moving averages of the magnetic fields, was developed.

During a test period when there were 97 AEs recorded by the plant computer (based on the usual voltage increase), the anode current measurement system detected 63 imminent AEs in advance of the voltage increase by times ranging from 5 seconds to more than one hour. It is anticipated that further refinement of the algorithm will improve these warnings and reduce the number of false alarms.

Knowledge of the currents of individual anodes has allowed conclusions to be drawn concerning the distribution of alumina in the pots. Tests have been carried out when three of the four alumina feeders have been turned off and the subsequent evolution of the anode currents (fields) was followed. The areas of the pot fed by each feeder have become apparent and it is suggested that individual anode current measurements will provide a method to optimize the feeding strategy. Further analysis may provide helpful information to verify if every feeder is working as expected during normal operation.

References

1. Evans, J.W., A. Lutzerath, and R. Victor, *On-line monitoring of anode currents; Experience at Trimet*, in *TMS - Light Metals* 2014: San Diego, CA. p. 739-742.
2. Evans, J.W. and N. Urata. *Technical and operational benefits of individual anode current monitoring.* in *10th Australasian aluminium smelting conference.* 2011. Lauceston, Tasmania.
3. Tarcy, G.P. and A.T. Tabereaux, *The initiation, propagation and termination of anode effects in Hall-Heroult cells*, in *TMS - Light metals*, S. Lindsay, Editor 2011. p. 329-332.
4. Kvande, H., et al., *Pseudo Resistance Curves for Aluminium Cell Control - Alumina Dissolution and Cell Dynamics*, in *TMS - Light Metals*, R. Huglen, Editor 1997.
5. Grjotheim, K. and B. Welch, *Aluminium Smelter Technology.* 2nd edition. 1988, Dusseldorf, Germany: Aluminium-Verlag.
6. Feng, Y., M. Cooksey, and P. Schwarz, *CFD Modelling of alumina mixing in aluminium reduction cells*, in *TMS - Light metals*, S. Lindsay, Editor 2011. p. 543-548.
7. Hofer, T., *Numerical simulation and optimization of the alumina distribution in an aluminium electrolysis pot*, in *Sciences de Base - Chaire d'analyses et de simulations numériques* 2011, École polytechnique fédérale de Lausanne: Lausanne. 121 pages.
8. Moxnes, B.P., et al., *Improved cell operation by redistribution of the alumina feeding*, in *TMS - Light metals*, G. Bearne, Editor 2009. p. 461-466.
9. Coursol, P., et al., *The transition strategy at Alouette towards higher productivity with a lower energy consumption*, in *TMS - Light metals*, C. Suarez, Editor 2012. p. 591-595.
10. Severo S., D., et al., *Comparison of various methods for modeling the metal-bath interface*, in *TMS - Light metals*, D. DeYoung, Editor 2008.